

# Thermo-elastic mismatch in nonhomogeneous beams

Alberto Carpinteri · Marco Paggi

Received: 9 January 2007 / Accepted: 1 January 2008 / Published online: 23 January 2008  
© Springer Science+Business Media B.V. 2008

**Abstract** The problem of thermo-elastic stress analysis in multi-layered nonhomogeneous beams is considered. The proposed analytical approach based on the multi-layered beam theory permits to take into account an arbitrary distribution of the Young's modulus, of the thermal-expansion coefficient, and of the temperature variation along the beam depth. The effect of shear deformability of the interfaces is also carefully analyzed. Useful closed-form solutions for the normal stresses in the layers and for the interface tangential stresses are provided in the case of nonhomogeneous bi- and tri-layered beams. The obtained results show the effectiveness of using functionally graded materials to relieve stress-concentrations due to the thermo-elastic mismatch typical of laminated beams with homogeneous layers.

**Keywords** Analytical approach · Functionally graded materials · Multi-layered beams · Thermo-elasticity · Thermo-elastic mismatch

## 1 Introduction

The analysis of thermo-elastic stresses in composite beams with homogeneous layers can be traced back to the pioneering work of Timoshenko [1]. On the basis of an elementary beam theory, he determined the normal stresses in the layers, assuming that these stresses remain unchanged along the longitudinal beam axis. As regards the interfacial stresses, it was just mentioned that they are of local type and concentrate near the strip ends at a distance comparable with the strip thicknesses. After that, various simplified approaches to the problem in question were suggested in the last decades, most in connection with the needs of the micro-electronics technology. Suhir [2,3] extended the Timoshenko solution by considering deformable interfaces. Introducing both the longitudinal and the transverse interfacial compliances, he evaluated the magnitude and distribution of the shearing and normal (peeling) stresses along the interface of bi-metal thermostats.

More recently, the Suhir solution was improved in [4], where a correction to the peeling stresses was proposed in order to satisfy the translation equilibrium in the direction normal to the layers. The discrepancies between the Suhir solution and the finite-element results were also analyzed in [5], where further corrections were proposed. An extension of this approach to electronic assemblies composed of three layers was proposed in [6], although the

---

A. Carpinteri · M. Paggi (✉)  
Department of Structural Engineering and Geotechnics, Politecnico di Torino, Corso Duca degli Abruzzi 24, 10129 Torino, Italy  
e-mail: marco.paggi@polito.it

thickness of the intermediate layer, i.e., the adhesive one, was considered much smaller than those of the adjacent layers. A general theory for the analysis of interfacial stresses in multi-layered homogeneous beams was recently discussed in [7,8], although the applications regarded electronic packaging with three layers only.

Due to the recent advances in materials science and technology, it is important to note that the corresponding problem in nonhomogeneous beams has received only minor attention as compared to its homogeneous counterpart. The production of functionally graded materials (FGM) has now made possible the realization of nonhomogeneous layers. Such materials consist of two phases of synthesized materials designed in such a way that the volume fractions of the constituents vary continuously along the layer depth to give a predetermined composition profile (see e.g. [9–18] for a detailed overview). The potentials of these new material microstructures are still under investigation by the scientific community. From a historical point of view, the FGM concept was proposed in 1984 as a way of preparing super heat-resistant materials for the spacecraft industry. Since the structural components of spacecrafts are exposed to high heat load, the material has to withstand severe thermo-mechanical loading. As a technical solution, a FGM was produced by using heat-resistant ceramics on the high-temperature side and tough metals with high thermal conductivity on the low-temperature side. The gradient composition at the interface can effectively relax the thermal-stress concentrations caused by the thermo-elastic mismatch [19].

The problem of heat conduction in nonhomogeneous materials was mathematically addressed in [20,21], where an improved expression for the heat-conduction equation was determined by considering temperature-dependent mechanical parameters. Concerning the analysis of thermo-elastic stresses in FGMs, recent studies deal with the behavior of thick plates with nonhomogeneous composition along their thickness [22]. The problem of thermal loading in bi-layered and/or FGM beams was investigated in [23]. Special emphasis was given to the analysis of the residual stress field induced by a hot bonding. The important problems of delamination, fatigue, and the related size effects were also addressed.

In this paper we propose a generalization of the analytical approach recently developed in [23] for the thermo-elastic stress analysis of multi-layered and/or FGM beams. With respect to the previous contributions, the proposed analytical approach based on the multi-layered beam theory permits to deal with a generic number of layers with an arbitrary grading on the Young's modulus and on the thermal-expansion coefficient. Moreover, a generic temperature distribution along the beam depth can be taken into account. Concerning the interfaces between two adjacent layers, two hypotheses are carefully examined: rigid interfaces and shear-deformable interfaces. The derived closed-form solutions are implemented in a code written in MATLAB<sup>®</sup>, which permits to automatically perform a thermo-elastic stress analysis of nonhomogeneous beams. This approach provides an easy-to-use estimation method for the interfacial stresses and presents several advantages with respect to the finite element approach. In fact, the application of the finite element method to functionally graded materials requires a special treatment of the mechanical properties variation [24]. This can be achieved today by using numerical techniques that are mainly restricted to research programmes, rather than implemented in commercial finite element software.

Numerical examples regarding bi- and tri-layered beams with nonhomogeneous properties are proposed. The obtained results demonstrate the effectiveness of FGMs in reducing the dangerous effects caused by the thermo-elastic mismatch at the interfaces.

## 2 Mathematical formulation

For the sake of generality, let us consider a composite beam consisting in  $n$  layers bonded together and subjected to a temperature excursion from a reference temperature,  $\Delta T(y)$  (see Fig. 1). In our formulation, the index  $i = 1, 2, \dots, n$  refers to the  $i$ th layer,  $h_i$  represents its thickness, whereas the width  $t$  is assumed to be constant throughout the whole beam depth. We set the origin ( $y=0$ ) of the coordinate system  $y$  at the extrados of the composite beam, i.e., at its upper surface.

The geometry of the beam and the thermal loading are symmetric with respect to the  $y$ -axis. In this stage, we admit an arbitrary dependence of the thermal conductivity and of the resulting  $\Delta T$  along the  $y$ -coordinate, since

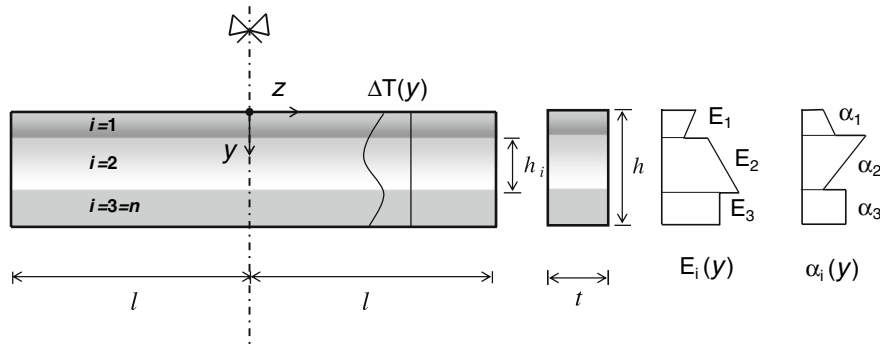


**Fig. 1** Scheme of the multi-layered nonhomogeneous beam analyzed in this study

the nonhomogeneous composition can affect not only the distribution of the elastic properties, but also the thermal conductivity entering the heat-conduction equation [20,21]. An arbitrary dependence of the Young’s modulus,  $E_i(y)$ , and of the thermal-expansion coefficient,  $\alpha_i(y)$ , on the  $y$ -coordinate is also considered.

Concerning the interfaces between two adjacent layers, two hypotheses are examined in the sequel: rigid interfaces and shear-deformable interfaces. In the former case, relative longitudinal displacements are not allowed at the interface and the normal stresses within the layers (along the longitudinal  $z$ -coordinate) are found to be the same in each transversal cross-section. The axial force supported by each layer is also independent of  $z$  and the tangential stresses are equal to zero along the interface, except at  $z = \pm l$  where they tend to infinity. In the latter configuration, the interfaces are assumed to be shear-deformable. This property is mathematically modeled by introducing a longitudinal interfacial compliance which describes the tangential behavior of the interface. In this case, the axial force of each layer is found to be dependent on the  $z$ -coordinate. The tangential stresses along the interfaces are different from zero near the free edges ( $z = \pm l$ ) where stress-concentrations are expected.

### 2.1 Rigid interfaces

The analysis of thermo-elastic stresses in multi-layered nonhomogeneous beams with rigid interfaces can be performed under the Euler–Bernoulli hypothesis of conservation of plane sections [20,25,26]. This implies that a generic plane section, which is perpendicular to the longitudinal axis of the beam before loading, still remains plane and perpendicular to this axis after deformation. Longitudinal fibers on the convex side are extended, whereas the fibers on the concave side are shortened. Clearly, there exists a plane where the fibers are not subjected to any elongation. This plane is referred to as the neutral plane and the intersection between this plane and any cross-section defines the neutral axis (see e.g. [25,26]).

As a consequence of this hypothesis on the beam deformation, the longitudinal strain,  $\varepsilon_z$ , is a linear function of the  $y$ -coordinate and the longitudinal displacements are continuous along the beam depth. The longitudinal strain at an arbitrary position  $y$  is given by:

$$\varepsilon_{z,i} = \alpha_i \Delta T_i + \frac{\sigma_{z,i}}{E_i} = \varepsilon_0 + \chi y, \tag{1}$$

where the parameters  $\varepsilon_0$  and  $\chi$  denote, respectively, the longitudinal strain and the beam curvature evaluated in correspondence of  $y = 0$ . Solving this equation for  $\sigma_{z,i}$ , we obtain:

$$\sigma_{z,i} = -\alpha_i E_i \Delta T_i + \varepsilon_0 E_i + \chi E_i y. \tag{2}$$

Therefore, the problem is reduced to finding  $\varepsilon_0$  and  $\chi$  for a given beam geometry and material distribution. To this end, we remark that the beam is completely free and exclusively subjected to a temperature variation from a reference temperature. Since external forces do not act on the layers, we can determine  $\varepsilon_0$  and  $\chi$  from the conditions of vanishing axial force and bending moment in a generic cross-section:

$$\sum_{i=1}^n \int_{y_i^{(1)}}^{y_i^{(2)}} \sigma_{z,i} t \, dy = 0, \quad \sum_{i=1}^n \int_{y_i^{(1)}}^{y_i^{(2)}} \sigma_{z,i} t y \, dy = 0, \tag{3a,b}$$

where  $y_i^{(1)}$  and  $y_i^{(2)}$  denote, respectively, the upper and the lower surfaces of the  $i$ th layer, their difference being equal to the layer thickness,  $h_i = y_i^{(2)} - y_i^{(1)}$ .

Introducing Eq. (2) into Eq. (3), we obtain the following equations:

$$\varepsilon_0 \sum_{i=1}^n \int_{y_i^{(1)}}^{y_i^{(2)}} E_i \, dy + \chi \sum_{i=1}^n \int_{y_i^{(1)}}^{y_i^{(2)}} E_i y \, dy = \sum_{i=1}^n \int_{y_i^{(1)}}^{y_i^{(2)}} \alpha_i E_i \Delta T_i \, dy, \tag{4a}$$

$$\varepsilon_0 \sum_{i=1}^n \int_{y_i^{(1)}}^{y_i^{(2)}} E_i y \, dy + \chi \sum_{i=1}^n \int_{y_i^{(1)}}^{y_i^{(2)}} E_i y^2 \, dy = \sum_{i=1}^n \int_{y_i^{(1)}}^{y_i^{(2)}} \alpha_i E_i \Delta T_i y \, dy. \tag{4b}$$

This equation set can be written in the following matrix form:

$$\begin{bmatrix} M_{11} & M_{12} \\ M_{21} & M_{22} \end{bmatrix} \begin{Bmatrix} \varepsilon_0 \\ \chi \end{Bmatrix} = \begin{Bmatrix} V_1 \\ V_2 \end{Bmatrix}, \tag{5}$$

where the matrix and vector coefficients are given by:

$$M_{11} = \sum_{i=1}^n \int_{y_i^{(1)}}^{y_i^{(2)}} E_i \, dy, \quad M_{12} = M_{21} = \sum_{i=1}^n \int_{y_i^{(1)}}^{y_i^{(2)}} E_i y \, dy, \quad M_{22} = \sum_{i=1}^n \int_{y_i^{(1)}}^{y_i^{(2)}} E_i y^2 \, dy, \tag{6a,b,c}$$

$$V_1 = \sum_{i=1}^n \int_{y_i^{(1)}}^{y_i^{(2)}} \alpha_i E_i \Delta T_i \, dy, \quad V_2 = \sum_{i=1}^n \int_{y_i^{(1)}}^{y_i^{(2)}} \alpha_i E_i \Delta T_i y \, dy. \tag{6d,e}$$

It is important to note that the matrix coefficients  $M_{ij}$  depend on the grading of the elastic moduli and on the layers' arrangement. On the other hand, the vector coefficients  $V_i$  depend not only on the grading of the elastic moduli, but also on the grading of the thermal-expansion coefficients.

Focusing our attention on the case of a uniform temperature variation, i.e.,  $\Delta T_i(y) = \Delta T$ , and a linear grading of the Young's moduli and of the thermal-expansion coefficients, the integrals in Eq. (6) can be performed in closed-form and we have:

$$M_{11} = \sum_{i=1}^n \bar{E}_i h_i, \tag{7a}$$

$$M_{12} = M_{21} = \sum_{i=1}^n \frac{1}{2} \left( E_i^{(1)} h_i - \Delta E_i \sum_{k=1}^{i-1} h_k \right) \left( 2 \sum_{k=1}^{i-1} h_k + h_i \right) + \frac{\Delta E_i}{3} \left[ 3 \left( \sum_{k=1}^{i-1} h_k \right)^2 + h_i^2 + 3 h_i \sum_{k=1}^{i-1} h_k \right] \tag{7b}$$

$$M_{22} = \sum_{i=1}^n \frac{1}{3} \left( E_i^{(1)} h_i - \Delta E_i \sum_{k=1}^{i-1} h_k \right) \left[ 3 \left( \sum_{k=1}^{i-1} h_k \right)^2 + h_i^2 + 3 h_i \sum_{k=1}^{i-1} h_k \right] + \frac{\Delta E_i}{4} \left( h_i + 2 \sum_{k=1}^{i-1} h_k \right) \left[ 2 \left( \sum_{k=1}^{i-1} h_k \right)^2 + h_i^2 + 2 h_i \sum_{k=1}^{i-1} h_k \right], \tag{7c}$$

$$V_1 = \Delta T \sum_{i=1}^n \left[ E_i^{(1)} \alpha_i^{(1)} h_i - E_i^{(1)} \Delta \alpha_i \sum_{k=1}^{i-1} h_k - \Delta E_i \alpha_i^{(1)} \sum_{k=1}^{i-1} h_k + \Delta E_i \Delta \alpha_i \frac{\left( \sum_{k=1}^{i-1} h_k \right)^2}{h_i} \right]$$

$$\begin{aligned}
 & + \frac{1}{2} \left( E_i^{(1)} \Delta\alpha_i + \Delta E_i \alpha_i^{(1)} - 2\Delta E_i \Delta\alpha_i \frac{\sum_{k=1}^{i-1} h_k}{h_i} \right) \left( h_i + 2 \sum_{k=1}^{i-1} h_k \right) \\
 & + \frac{\Delta E_i \Delta\alpha_i}{3h_i} \left[ 3 \left( \sum_{k=1}^{i-1} h_k \right)^2 + h_i^2 + 3h_i \sum_{k=1}^{i-1} h_k \right], \tag{7d}
 \end{aligned}$$

$$\begin{aligned}
 V_2 = \Delta T \sum_{i=1}^n & \left[ E_i^{(1)} \alpha_i^{(1)} h_i - E_i^{(1)} \Delta\alpha_i \sum_{k=1}^{i-1} h_k - \Delta E_i \alpha_i^{(1)} \sum_{k=1}^{i-1} h_k + \Delta E_i \Delta\alpha_i \frac{\left( \sum_{k=1}^{i-1} h_k \right)^2}{h_i} \right] \\
 & \times \frac{h_i + 2 \sum_{k=1}^{i-1} h_k}{2} + \frac{1}{3} \left[ E_i^{(1)} \Delta\alpha_i + \Delta E_i \alpha_i^{(1)} - 2\Delta E_i \Delta\alpha_i \frac{\sum_{k=1}^{i-1} h_k}{h_i} \right] \\
 & + \left[ 3 \left( \sum_{k=1}^{i-1} h_k \right)^2 + h_i^2 + 3h_i \sum_{k=1}^{i-1} h_k \right] + \frac{\Delta E_i \Delta\alpha_i}{4h_i} \left( h_i + 2 \sum_{k=1}^{i-1} h_k \right) \\
 & \times \left[ 2 \left( \sum_{k=1}^{i-1} h_k \right)^2 + h_i^2 + 2h_i \sum_{k=1}^{i-1} h_k \right], \tag{7e}
 \end{aligned}$$

where  $\bar{E}_i$  denotes the average Young’s modulus in the  $i$ th layer. The Young’s moduli,  $E_i$ , and the thermal-expansion coefficients,  $\alpha_i$ , have the following expressions:

$$E_i(y) = E_i^{(1)} + \frac{1}{h_i} \left( y - \sum_{k=1}^{i-1} h_k \right) \Delta E_i, \quad \alpha_i(y) = \alpha_i^{(1)} + \frac{1}{h_i} \left( y - \sum_{k=1}^{i-1} h_k \right) \Delta\alpha_i, \tag{8a,b}$$

where  $\Delta E_i = E_i^{(2)} - E_i^{(1)}$  and  $\Delta\alpha_i = \alpha_i^{(2)} - \alpha_i^{(1)}$  denote, respectively, the Young’s modulus and the thermal-expansion coefficient variations within each layer from the upper interface, with superscript (1), to the lower one, with superscript (2). Note that the summations in Eq. (8) are different from zero if and only if the index  $i$  is greater than unity.

It is important to remark that the normal stresses computed according to this formulation are independent of the  $z$ -coordinate. As a consequence, the axial force supported by each layer,  $N_i$ , is also constant along the  $z$ -coordinate and the tangential stresses along the interfaces are equal to zero. At the emerging points of the interface with the free boundary ( $z = \pm l$ ), the tangential stresses tend theoretically to infinity and the order of the stress singularity has to be determined according to an asymptotic analysis (see e.g. the mathematical methods proposed in [27,28]).

### 2.2 Shear-deformable interfaces

In the present section we analyze the case of shear-deformable interfaces, where relative displacements are admitted from one layer to another. Also in this case, we consider a geometric symmetry with respect to the  $y$ -axis and a temperature variation,  $\Delta T_i(y)$ , dependent only on the  $y$ -coordinate.

Under these conditions, relative displacements build up along the interfaces and the axial forces in the layers,  $N_i$ , which represent the integral of the normal stresses along the layer cross-section, become functions of the  $z$ -coordinate. It is important to remark that, owing to the symmetry of the problem, the axial forces and the normal stresses computed at  $z = 0$  correspond to those computed in the case of rigid interfaces. This is due to the vanishing relative displacements between the layers in this cross-section.

The axial equilibrium along the longitudinal coordinate provides the tangential stresses along the interfaces ( $i = 2, \dots, n - 1$ ):

$$\tau_{1,2} = -\frac{1}{t} \frac{dN_1(z)}{dz}, \quad \tau_{i,i+1} - \tau_{i-1,i} = -\frac{1}{t} \frac{dN_i(z)}{dz}, \quad \tau_{n-1,n} = \frac{1}{t} \frac{dN_n(z)}{dz}, \tag{9a,b,c}$$



$$[C] = \begin{bmatrix} \alpha_1^{(2)} & & & & & \\ & \ddots & & & & \\ & & \alpha_i^{(1)} & & & \\ & & & \alpha_i^{(2)} & & \\ & & & & \ddots & \\ & & & & & \alpha_n^{(1)} \end{bmatrix}. \tag{16}$$

Note that the rotational equilibrium is not imposed in this formulation. An exact treatment of the problem would require the use of coefficients  $k_i^{(j)}$  dependent on the longitudinal coordinate. In any case, it is important to note that the rotational equilibrium is a priori satisfied in the case of bi-layered beams. In this instance, in fact, the analysis of the free-body diagram of each layer imposes that the corresponding axial force must be applied at the interface level for any value of the  $z$ -coordinate. As a consequence of this condition, the distribution of the normal stresses in the layers,  $\sigma_z(y)$ , is simply rescaled by a factor of proportionality with respect to that computed at  $z = 0$ . Therefore, the coefficients  $k_i^{(j)}$  turn out to be independent of the longitudinal coordinate and the solution is exact. When more than two layers are taken into account, the intermediate layers are not in equilibrium. However, as will be shown in the numerical examples, the resulting approximation can be considered acceptable from an engineering point of view.

The compatibility equation can be written by observing that the relative displacement at the interface between two adjacent layers corresponds to the shearing deformation of the interface, which is characterized by a given compliance. This compliance is usually experimentally related to the thickness of the adhesive,  $h_a$ , and to its shear modulus,  $G$ . In formulae we have:

$$w_{i+1}^{(1)}(z) - w_i^{(2)}(z) = h_a \gamma(z) = h_a \frac{\tau_{i,i+1}}{G}, \quad i = 1, \dots, n - 1. \tag{17}$$

In matrix form we have the following expression:

$$\begin{matrix} \{\tau\} & = & \frac{G}{h_a} & [D] & \{w\}, \\ (n-1) \times 1 & & & (n-1) \times 2(n-1) & 2(n-1) \times 1 \end{matrix} \tag{18}$$

where the matrix  $[D]$  is given by:

$$[D] = \begin{bmatrix} -1 & 1 & & & & \\ & -1 & 1 & & & \\ & & & \ddots & & \\ & & & & \ddots & \\ & & & & & -1 & 1 \\ & & & & & & -1 & 1 \end{bmatrix}. \tag{19}$$

It is important to notice that, when the thickness of the adhesive vanishes, the model predicts unbounded tangential stresses, as also observed in the case of perfectly bonded zero-thickness interfaces [27].

Introducing Eqs. (18) and (14) into Eq. (10), it is possible to obtain an equation set consisting in  $n$  integro-differential equations in  $n$  unknowns, which are represented by the values of the axial forces supported by each layer,  $N_i$ :

$$\frac{d}{dz} \{N\} + K[A][D][B] \int_0^z \{N\} d\xi + K[A][D][C] \{\Delta T\} z = \{0\}, \tag{20}$$

where the parameter  $K$  denotes  $Gt/h_a$ . To solve the problem, the equation set (20) has to be differentiated with respect to  $z$  in order to obtain pure ODEs:

$$\frac{d^2}{dz^2} \{N\} + K[A][D][B]\{N\} + K[A][D][C]\{\Delta T\} = \{0\}. \tag{21}$$

Finally, after some manipulation and considering the equilibrium equation (12), it is possible to express the  $N_i$  unknowns in terms of the axial force of a given layer, say  $N_j$ . This procedure yields a single ODE in the unknown  $N_j$  which has to be integrated by considering suitable boundary conditions.

To fix ideas, let us consider as a representative example the case of two layers, which was also analyzed in [23]. In this case, we have only one compatibility equation:

$$k_2^{(1)} \int_0^z \frac{N_2(\xi)}{E_2^{(1)} A_2} d\xi - k_1^{(2)} \int_0^z \frac{N_1(\xi)}{E_1^{(2)} A_1} d\xi + \alpha_2^{(1)} \Delta T_2^{(1)} z - \alpha_1^{(2)} \Delta T_1^{(2)} z = \frac{h_a}{G} \tau_{1,2}. \tag{22}$$

Considering the longitudinal equilibrium of the beam ( $N_2 = -N_1 = N$ ) and the equilibrium equation (9a), we finally obtain a single integro-differential equation in the unknown  $N$ :

$$k_1^{(2)} \int_0^z \frac{N(\xi)}{E_1^{(2)} A_1} d\xi + k_2^{(1)} \int_0^z \frac{N(\xi)}{E_2^{(1)} A_2} d\xi + \alpha_2^{(1)} \Delta T_2^{(1)} z - \alpha_1^{(2)} \Delta T_1^{(2)} z = \frac{1}{K} \frac{dN(z)}{dz}. \tag{23}$$

Differentiation of this equation with respect to  $z$  provides the following second-order ODE:

$$\frac{d^2 N}{dz^2} + \beta_*^2 N + \gamma_* = 0, \tag{24}$$

where

$$\beta_*^2 = -K \left( \frac{k_1^{(2)}}{E_1^{(2)} A_1} + \frac{k_2^{(1)}}{E_2^{(1)} A_2} \right), \quad \gamma_* = K \left( \alpha_2^{(1)} \Delta T_2^{(1)} - \alpha_1^{(2)} \Delta T_1^{(2)} \right).$$

The integral of this ODE is given by:

$$N(z) = C_1 e^{\beta_* z} + C_2 e^{-\beta_* z} - \frac{\gamma_*}{\beta_*^2}, \tag{25}$$

where the constants  $C_1$  and  $C_2$  have to be determined by imposing the boundary conditions. In this problem, they are represented by the symmetry condition in  $z = 0$  and by the fact that axial forces have to be equal to zero at  $z = \pm l$ :

$$\frac{dN}{dz}(z = 0) = 0, \quad N(z = \pm l) = 0. \tag{26a,b}$$

Therefore, the constants can be determined and are equal to:

$$C_1 = C_2 = \frac{\gamma_*}{2\beta_*^2 \cosh(\beta_* l)}. \tag{27}$$

In the case of three layers, the governing equations become more complicated. Since we have two interfaces, the compatibility equations are ( $N_3 = -N_1 - N_2$ ):

$$k_1^{(2)} \int_0^z \frac{N_1}{E_1^{(2)} A_1} d\xi - k_2^{(1)} \int_0^z \frac{N_2}{E_2^{(1)} A_2} d\xi + \alpha_1^{(2)} \Delta T_1^{(2)} z - \alpha_2^{(1)} \Delta T_2^{(1)} z = \frac{1}{K} \frac{dN_1}{dz} \tag{28a}$$

$$k_3^{(1)} \int_0^z \frac{N_1 + N_2}{E_3^{(1)} A_3} d\xi + k_2^{(2)} \int_0^z \frac{N_2}{E_2^{(2)} A_2} d\xi + \alpha_2^{(2)} \Delta T_2^{(2)} z - \alpha_3^{(1)} \Delta T_3^{(1)} z = \frac{1}{K} \frac{d(N_1 + N_2)}{dz} \tag{28b}$$

Differentiation of Eqs. (28) with respect to  $z$  permits to obtain two second-order ODE in the unknowns  $N_1$  and  $N_2$ . Taking the difference between the first and the second equation, it is possible to express  $N_1$  as a function of  $N_2$ :

$$N_1 = \frac{1}{K\phi} \frac{d^2 N_2}{dz^2} - \frac{1}{\phi} \left( \frac{k_2^{(1)}}{E_2^{(1)} A_2} + \frac{k_3^{(1)}}{E_3^{(1)} A_3} + \frac{k_2^{(2)}}{E_2^{(2)} A_2} \right) N_2 - \frac{1}{\phi} \left( \alpha_2^{(1)} \Delta T_2^{(1)} - \alpha_1^{(2)} \Delta T_1^{(2)} + \alpha_2^{(2)} \Delta T_2^{(2)} - \alpha_3^{(1)} \Delta T_3^{(1)} \right), \tag{29}$$

where the symbol  $\phi$  denotes:

$$\phi = \frac{k_3^{(1)}}{E_3^{(1)} A_3} - \frac{k_1^{(2)}}{E_1^{(2)} A_1}. \tag{30}$$

Finally, Eq. (29) can be introduced into Eq. (28a) to determine a fourth-order ODE in the unknown  $N_2$ :

$$N_2^{IV} + \beta N_2^{II} + \delta N_2 + \gamma = 0, \tag{31}$$

where the constant coefficients  $\beta$ ,  $\delta$  and  $\gamma$  are:

$$\beta = -K \left( \frac{k_2^{(1)}}{E_2^{(1)} A_2} + \frac{k_3^{(1)}}{E_3^{(1)} A_3} + \frac{k_2^{(2)}}{E_2^{(2)} A_2} + \frac{k_1^{(2)}}{E_1^{(2)} A_1} \right), \tag{32a}$$

$$\delta = K^2 \left[ \phi \left( \frac{k_2^{(1)}}{E_2^{(1)} A_2} \right) + \frac{k_1^{(2)}}{E_1^{(2)} A_1} \left( \frac{k_2^{(1)}}{E_2^{(1)} A_2} + \frac{k_3^{(1)}}{E_3^{(1)} A_3} + \frac{k_2^{(2)}}{E_2^{(2)} A_2} \right) \right], \tag{32b}$$

$$\gamma = K^2 \left[ \phi \left( \alpha_2^{(1)} \Delta T_2^{(1)} - \alpha_1^{(2)} \Delta T_1^{(2)} \right) + \frac{k_1^{(2)}}{E_1^{(2)} A_1} \left( \alpha_2^{(1)} \Delta T_2^{(1)} - \alpha_1^{(2)} \Delta T_1^{(2)} + \alpha_2^{(2)} \Delta T_2^{(2)} - \alpha_3^{(1)} \Delta T_3^{(1)} \right) \right]. \tag{32c}$$

The solution to this ODE is given by:

$$N_2(z) = C_1 e^{\lambda_1 z} + C_2 e^{\lambda_2 z} + C_3 e^{\lambda_3 z} + C_4 e^{\lambda_4 z} - \frac{\gamma}{\delta}, \tag{33}$$

where the exponents  $\lambda_k$  ( $k = 1, \dots, 4$ ) are:

$$\lambda_{1,2} = \sqrt{\frac{-\beta \pm \sqrt{\beta^2 - 4\delta}}{2}}, \quad \lambda_{3,4} = -\sqrt{\frac{-\beta \pm \sqrt{\beta^2 - 4\delta}}{2}}. \tag{34}$$

The constants  $C_k$  ( $k = 1, \dots, 4$ ) have to be determined by imposing the boundary conditions. Also in this case, they are represented by the symmetry condition at  $z = 0$  and by the fact that axial forces are equal to zero at  $z = \pm l$ :

$$\frac{dN_1}{dz}(z = 0) = 0, \quad \frac{dN_2}{dz}(z = 0) = 0, \quad N_1(z = \pm l) = 0, \quad N_2(z = \pm l) = 0. \tag{35a,b,c,d}$$

Therefore, these boundary conditions involve not only  $N_2$  and its first derivative, as in the previous case, but also its second and third derivatives due to the boundary conditions imposed on the function  $N_1$ ; see Eq. (29). When the functions  $N_i(z)$  are determined, the tangential stresses can be computed according to Eq. (9).

This procedure, performed in detail for the problems consisting in two or three layers, can be repeated for multi-layered beams with a higher number of layers. In general, we note that, for a multi-layered beam with  $n$  layers, the order of the governing ODE that has to be solved becomes equal to  $2(n - 1)$ , i.e., it is twice the number of interfaces.

### 3 Numerical examples

The determination of normal and tangential stresses according to the mathematical formulation presented in the previous sections has been obtained using MATLAB. The realized code permits to perform a thermo-elastic stress analysis of a nonhomogeneous beam with an arbitrary number of layers with piece-wise linearly variable Young’s moduli and thermal-expansion coefficients. A generic temperature distribution can also be prescribed. Numerical examples concerning bi-layered and tri-layered beams are shown in the sequel.

#### 3.1 Bi-layered nonhomogeneous beams

Let us consider a bi-layered beam with constant elastic and thermal properties in each layer, but different from the first layer to the second one (see Fig. 2a).

As an example, we consider a bi-layered beam composed of Tungsten (W) as the material (1) and a mixture of Nickel and Steel (Ni-Fe) as the material (2). The geometrical parameters are:  $h_1 = h_2 = 1 \times 10^{-3}$  m,  $l = 1 \times 10^{-2}$  m and  $t = 1 \times 10^{-3}$  m. The beam is subjected to a uniform temperature excursion,  $\Delta T = 500$  K, and the mechanical parameters are [29]:  $E_1 = 400$  GPa,  $\alpha_1 = 5.3 \times 10^{-6}$ /K,  $E_2 = 255$  GPa and  $\alpha_2 = 15.0 \times 10^{-6}$ /K.

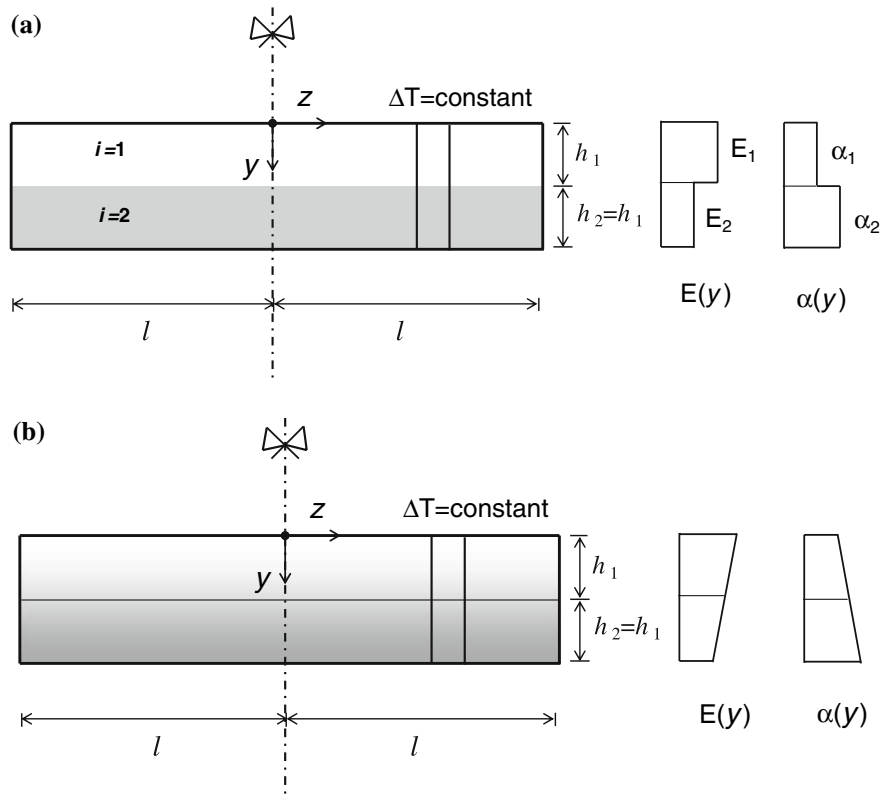


**Fig. 2** Schemes of two-layered nonhomogeneous beams. (a) Homogeneous composition in each layer, (b) Linear grading solution

Under these conditions, the thermo-elastic analysis in the case of rigid interfaces shows that the beam is subjected to both an axial deformation,  $\varepsilon_0 = 1.3 \times 10^{-3}$ , and a curvature,  $\chi = 3.59 \text{ m}^{-1}$ . The normal stress,  $\sigma_z$ , is shown in Fig. 3 as a function of the  $y$ -coordinate. Due to the thermo-elastic mismatch between the two layers, the normal stress is discontinuous in correspondence of the bi-material interface. It has to be noticed that, due to the axial equilibrium, the axial force in the lower layer is the opposite of that in the upper layer, i.e.,  $N_2 = -N_1 = N$ . Moreover, the rotational equilibrium imposes that these axial forces are both applied at the interface level for any value of the  $z$ -coordinate.

Tangential stresses along the interface can also be computed by considering a shear-deformable interface with  $G \cong (E_1 + E_2)/4$  and  $h_a = 1 \times 10^{-4} \text{ m}$ . Equation (25) provides the variation of the axial force  $N$  along the beam span (see Fig. 4a). As can be readily seen, the axial force is nearly constant from the symmetry axis ( $z = 0$ ), up to  $z/l \cong 0.9$ . Near the border,  $N$  tends rapidly to zero. As a consequence of this trend, the tangential stresses computed according to Eq. (9a) are equal to zero when  $N$  is constant and present a sudden increase in their modulus when  $z/l \cong 1$  (see Fig. 4b). Due to the finite interface thickness, the tangential stresses are always bounded along the beam length.

In this case study, the use of a linear grading on the Young's modulus and on the thermal-expansion coefficient can be very effective. For instance, if we consider a linearly variable material composition ranging from pure Tungsten at  $y = 0$  to pure Ni-Fe at  $y = h$ , then we obtain a single-layer FGM beam with  $E_1^{(1)} = 400 \text{ GPa}$ ,  $E_1^{(2)} = 255 \text{ GPa}$ ,  $\alpha_1^{(1)} = 5.3 \times 10^{-6}/\text{K}$  and  $\alpha_1^{(2)} = 15.0 \times 10^{-6}/\text{K}$  (see Fig. 2b).

A closed-form solution to the equation set (5) can be derived and we obtain  $\varepsilon_0 = \alpha_1^{(1)} \Delta T$  and  $\chi = (\Delta \alpha_1 \Delta T)/h$ . As a result, introducing these values into Eq. (2), the normal stresses are found to be equal to zero. It is interesting to note that this result is independent of the grading on the Young's modulus, since the solution vector  $(\varepsilon_0; \chi)^T$  does not depend on the parameters  $E_1^{(j)}$ .

**Fig. 3** Normal stresses along the beam depth for a bi-layered beam

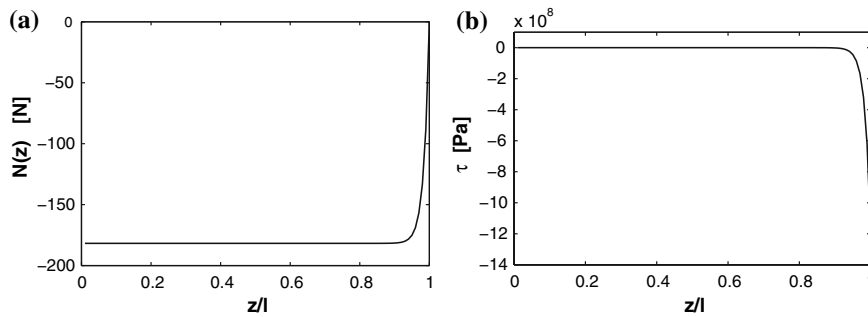
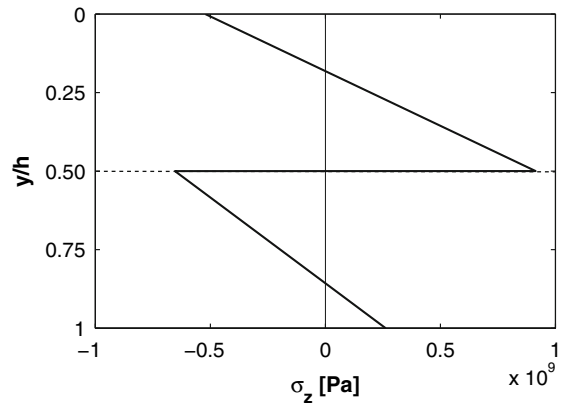


**Fig. 4** Axial force in the upper layer and tangential stresses vs. longitudinal coordinate for a bi-layered beam. (a) Axial force, (b) Tangential stresses

As a limit case, when  $\alpha_1^{(1)} = \alpha_1^{(2)}$ , and we have a grading on the Young’s modulus only, we obtain  $V_1 = M_{11}\alpha_1 \Delta T$ ,  $V_2 = M_{12}\alpha_1 \Delta T$ ,  $\chi = 0$  and  $\varepsilon_0 = \alpha_1 \Delta T$ , as for a classical homogeneous beam. Also in this case, both the normal and the tangential stresses are equal to zero in the whole beam.

### 3.2 Tri-layered nonhomogeneous beams

As a representative example, let us consider a tri-layered beam with homogeneous layers. The first and the third layers are composed, respectively, of Tungsten and Ni–Fe, whereas the intermediate layer has an average composition (see Fig. 5a). The thermo-elastic parameters are:  $E_1 = 400$  GPa,  $\alpha_1 = 5.3 \times 10^{-6}$ /K,  $E_2 = (255 + 400)/2$  GPa,  $\alpha_2 = (5.3 + 15.0) \times 10^{-6}/2$ , 1/K,  $E_3 = 255$  GPa and  $\alpha_3 = 15.0 \times 10^{-6}$ /K (see Fig. 5a). We consider a uniform temperature excursion,  $\Delta T = 500$  K, and the following geometrical parameters:  $h_1 = h_2 = h_3 = 1 \times 10^{-3}$  m,  $l = 1 \times 10^{-2}$  m and  $t = 1 \times 10^{-3}$  m. This tri-layered solution is also compared with that obtained using a FGM composing the intermediate layer to obtain a smooth transition from the upper to the lower material (see Fig. 5b).

The normal stresses computed according to the rigid-interface assumption are shown in Fig. 6 for these two configurations. As can be readily seen, the use of a FGM permits to remove the discontinuities in the normal stresses in correspondence of the interfaces. Moreover, the linear grading in the Young’s modulus and in the thermal-expansion coefficient in the intermediate layer results in a quadratic variation of the normal stresses for  $h_1 \leq y \leq h_1 + h_2$  (see Eq. (2)).

Another important difference between the two solutions regards the values of the axial force in each layer. For the multi-layered solution with homogeneous properties, the axial forces  $N_i$  ( $i = 1, \dots, 3$ ) are different in the layers, provided that  $\sum_{k=1}^3 N_k = 0$  (see Fig. 6a). When the FGM solution is adopted (see Fig. 6b), the axial forces are equal to zero in each layer. This observation is fully consistent with the predictions of the theoretical model for shear-deformable interfaces. In fact, when the temperature excursion is the same in each layer and the

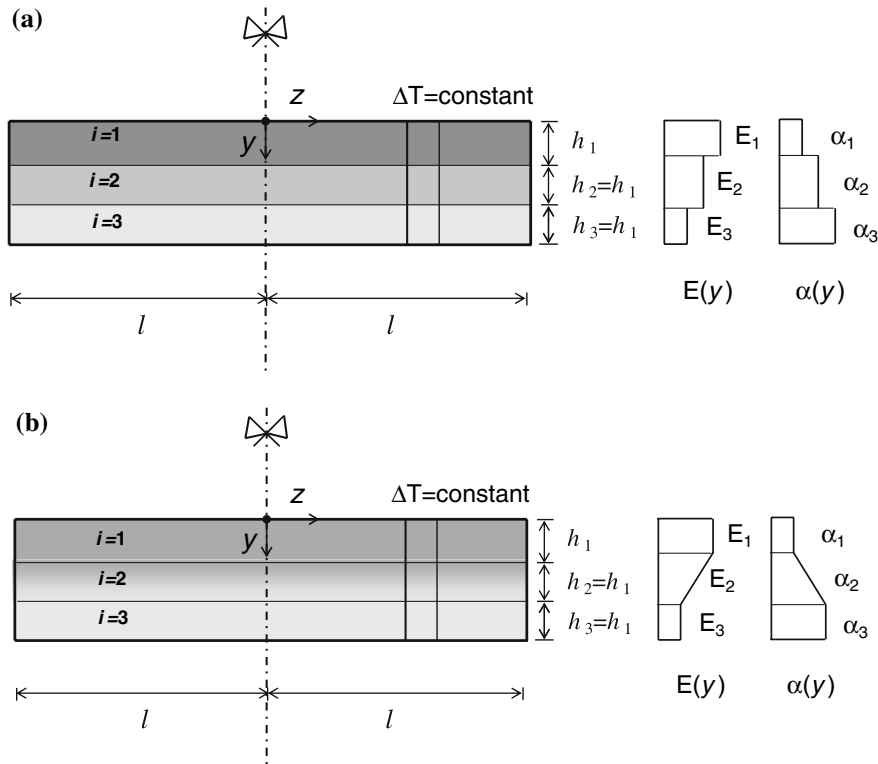


**Fig. 5** Schemes of tri-layered nonhomogeneous beams. (a) Homogeneous composition in each layer, (b) linear grading in the intermediate layer

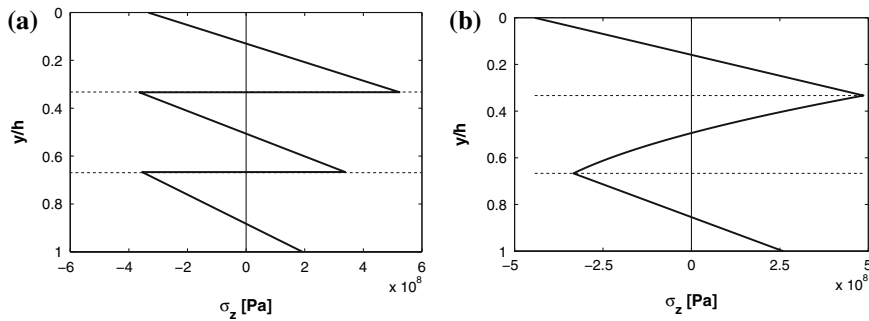


**Fig. 6** Normal stresses along the beam depth for a tri-layered beam. (a) Tri-layered beam, (b) tri-layered beam with a FGM interlayer

thermal-expansion coefficients are continuous along the interfaces, the constant  $\gamma$  in Eq. (31) is equal to zero. As a result, the ODE (31) provides  $N_2 = 0$ . The axial force  $N_1$  computed according to Eq. (29) becomes equal to zero in its turn and, from the longitudinal equilibrium, we have also  $N_3 = 0$ . As a consequence, the tangential forces along the interfaces are equal to zero. Moreover, the rotational equilibrium is always satisfied, the normal-stress distribution being the same for any value of the  $z$ -coordinate.

In the case of homogeneous layers, Eq. (33) with the boundary conditions (35) permit to determine the axial forces in each layer as functions of the  $z$ -coordinate (see Fig. 7a). Finally, the tangential stresses along the two interfaces can be computed according to Eq. (9) and are shown in Fig. 7b in the range  $0.9 \leq z/l \leq 1.0$ . Due to the fact that  $N_3$  is less than  $N_1$ , the maximum tangential stress along the second interface is lower than that on the first interface.

In this case, as mentioned in the previous section, the rotational equilibrium of the intermediate layer is no longer exactly satisfied. However, the error is a rapidly decreasing function of the thickness of the intermediate layer. A

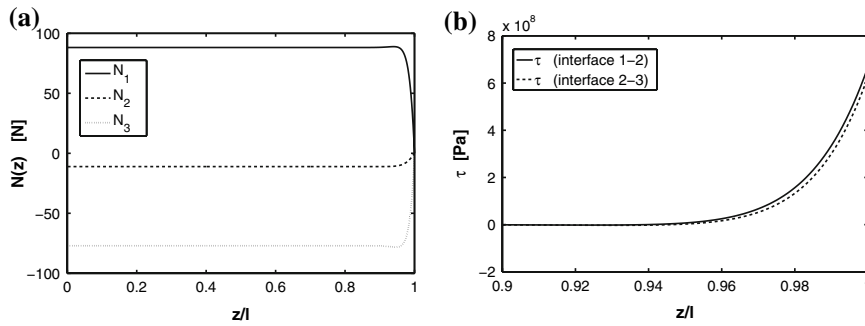
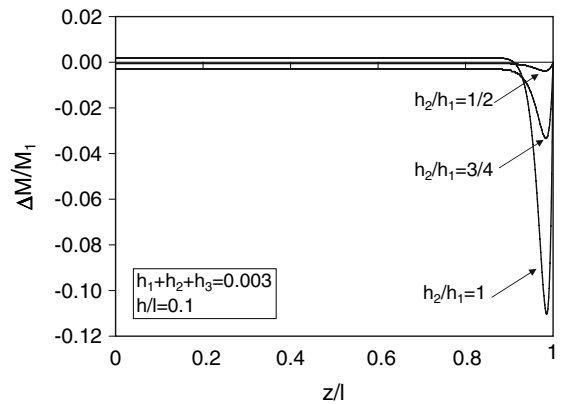


**Fig. 7** Axial forces and tangential stresses vs. longitudinal coordinate for a tri-layered beam. **(a)** Axial forces, **(b)** tangential stresses ( $0.9 \leq z/l \leq 1$ )

**Fig. 8** Out-of-balance in the rotational equilibrium as a function of the longitudinal coordinate



measure of the out-of-balance in the equilibrium equation is simply given by the sum of the bending moments supported by the layers,  $\sum_{i=1}^3 M_i = \Delta M$ . This quantity, nondimensionalized with respect to the bending moment supported by the first layer,  $M_1$ , is shown in Fig. 8 as a function of the longitudinal coordinate. Three configurations are considered, each one characterized by a different value of the relative thickness of the intermediate layer with respect to that of the first layer,  $h_2/h_1$ . In the simulations we have kept the following parameter constants:  $h_1 = h_3$ ,  $h = 0.003$  m and  $h/l = 1/10$ . As can be readily seen, the out-of-balance in the equilibrium equation becomes less than 3% of the bending moment supported by the first layer for  $h_2/h_1 \lesssim 3/4$ . This error can be considered acceptable from an engineering point of view, since the thickness of the intermediate layer is usually much smaller than those of the adjacent layers in practical applications.

#### 4 Conclusion

In this paper, we have presented an analytical approach based on the multi-layered beam theory for the thermo-elastic analysis of nonhomogeneous beams subjected to a generic temperature variation from a reference value along their depths. The proposed analytical solutions constitute a step forward with respect to previous thermo-elastic studies on nonhomogeneous beams. The proposed formulation, in fact, can deal with a generic number of layers and can consider either rigid or shear-deformable interfaces.

According to this approach, some important numerical examples are provided for bi- and tri-layered beams. In the former situation, a grading of the elastic modulus and of the thermal-expansion coefficient allows to relieve the normal stresses along the beam. In the latter, the use of a FGM intermediate layer connecting two homogeneous layers permits to relieve the interface tangential stresses.

Another important application of this approach concerns the analysis of residual stresses that are generated during the bonding process. In fact, from a theoretical point of view, the problem of residual stresses induced by a hot bonding of  $n$  material components during the fabrication process can be considered equivalent, neglecting the algebraic sign, to the problem of thermal stresses induced by a temperature increase in an already bonded multi-layered structure [30]. As a consequence, the problem of residual stresses induced in the elements by a temperature increase  $\Delta T$  can be studied as a problem of thermal stresses due to a temperature decrease of the same amount.

**Acknowledgements** The financial support provided by the European Community to the Leonardo da Vinci ILTOF Project (Innovative Learning and Training on Fracture) is gratefully acknowledged. The authors would like to thank Prof. V.V. Meleshko for his kind invitation to participate in this Special Issue.

## References

1. Timoshenko SP (1925) Analysis of bi-metal thermostats. *J Opt Soc Am* 11:233–255
2. Suhir E (1986) Stresses in bi-metal thermostats. *ASME J Appl Mech* 53:657–660
3. Suhir E (1989) Interfacial stresses in bimetal thermostats. *ASME J Appl Mech* 56:595–600
4. Jiang Q, Huang Y, Chandra A (1997) Thermal stresses in layered electronic assemblies. *ASME J Electron Packaging* 119:127–132
5. Tsai MY, Hsu CH, Han CN (2004) A note on Suhir's solution of thermal stresses for a die-substrate assembly. *ASME J Electron Packaging* 126:115–119
6. Wang K, Huang Y, Chandra A, Hu KX (2000) Interfacial shear stresses, peeling stresses, and die cracking stress in trilayer electronic assemblies. In: The seventh intersociety conference on thermal and thermomechanical phenomena in electronic systems, ITherm 2000, vol 2, pp 56–64
7. Wen Y, Basaran C (2003) Thermal stress analysis of multilayered microelectronic packaging. *ASME J Electron Packaging* 125:134–138
8. Wen Y, Basaran C (2004) An analytical model for thermal stress analysis of multi-layered microelectronic packaging. *Mech Mater* 36:369–385
9. Delale F, Erdogan F (1983) The crack problem for a nonhomogeneous plane. *ASME J Appl Mech* 50:609–614
10. Delale F (1985) Mode III fracture of bonded nonhomogeneous materials. *Eng Fract Mech* 22:213–226
11. Eischen J (1987) Fracture of nonhomogeneous materials. *Int J Frac* 34:3–22
12. Erdogan F (1995) Fracture mechanics of functionally gradient materials. *Composites Eng* 5:753–770
13. Jin Z-H, Batra R (1996) Some basic fracture mechanics concepts in functionally graded materials. *J Mech Phys Solids* 44:1221–1235
14. Erdogan F, Wu B (1997) The surface crack problem for a plate with functionally graded properties. *ASME J Appl Mech* 17:449–456
15. Paulino G (ed) (2002) Special issue on fracture of functionally graded materials, vol 69. *Engineering Fracture Mechanics*
16. Guler M, Erdogan F (2004) Contact mechanics of graded coatings. *Int J Solids Struct* 4:3865–3889
17. Carpinteri A, Paggi M (2005) On the asymptotic stress field in angularly nonhomogeneous materials. *Int J Fract* 135:267–283
18. Carpinteri A, Paggi M, Pugno N (2006) An analytical approach for fracture and fatigue in functionally graded materials. *Int J Fract* 141:535–547
19. Niino M, Maeda S (1990) Recent development status of functionally gradient materials. *ISIJ Int* 30:699–703
20. Noda N (1999) Thermal stresses in functionally graded materials. *J Therm Stresses* 22:477–512
21. Jin Z-H, Batra R (2006) Crack tip fields in functionally graded materials with temperature-dependent properties. *AIAA J* 44:2129–2130
22. Qian L, Batra R (2004) Transient thermoelastic deformations of a thick functionally graded plate. *J Therm Stresses* 27:705–740
23. Carpinteri A, Pugno N (2006) Thermal loading in multi-layered and/or functionally graded materials: residual stress field, delamination, fatigue and related size effects. *Int J Solids Struct* 43:828–841
24. Kim J-H, Paulino G (2002) Isoparametric graded finite elements for nonhomogeneous isotropic and orthotropic materials. *ASME J Appl Mech* 69:502–514
25. Carpinteri A (1997) *Structural mechanics: a unified approach*. E&FN Spon, London
26. Chawla K (1987) *Composite materials: science and engineering*. Springer-Verlag, New York
27. Munz D, Yang Y (1992) Stress singularities at the interface in bonded dissimilar materials under mechanical and thermal loading. *ASME J Appl Mech* 59:857–861
28. Munz D, Fett T, Yang Y (1993) The regular stress term in bonded dissimilar materials after a change in temperature. *Eng Fract Mech* 44:185–194
29. Batra R, Love B (2005) Crack propagation due to brittle and ductile failures in microporous thermoelastoviscoplastic functionally graded materials. *Eng Fract Mech* 72:1954–1979
30. Carpinteri A, Paggi M (2007) Numerical analysis of fracture mechanisms and failure modes in bi-layered structural components. *Finite Elem Anal Des* 43:941–953